

# Dealing with collinearity in large-scale linear system identification using Bayesian regularization

Wenqi Cao<sup>1</sup> and Gianluigi Pillonetto<sup>2</sup>

**Abstract**— We consider the identification of large-scale linear and stable dynamic systems whose outputs may be the result of many correlated inputs. Hence, severe ill-conditioning may affect the estimation problem. This is a scenario often arising when modeling complex physical systems given by the interconnection of many sub-units where feedback and algebraic loops can be encountered. We develop a strategy based on Bayesian regularization where any impulse response is modeled as the realization of a zero-mean Gaussian process. The stable spline covariance is used to include information on smooth exponential decay of the impulse responses. We then design a new Markov chain Monte Carlo scheme that deals with collinearity and is able to efficiently reconstruct the posterior of the impulse responses. It is based on a variation of Gibbs sampling which updates possibly overlapping blocks of the parameter space on the basis of the level of collinearity affecting the different inputs. Numerical experiments are included to test the goodness of the approach where hundreds of impulse responses form the system and inputs correlation may be very high.

## I. INTRODUCTION

Large-scale dynamic systems arise in many scientific fields like engineering, biomedicine and neuroscience [12], [15], [21], [30]. Modeling these complex physical systems is crucial for prediction and control purposes [18], [35]. They can be often interpreted as networks composed of a large set of interconnected sub-units. One can also describe them through many nodes which can communicate each other through modules driven by measurable inputs or noises [8], [19], [37], [40].

We will assume that linear dynamics underly our large-scale dynamic system focus on the identification of Multiple Inputs Single Output (MISO) models. Hence, system impulse responses have to be estimated from input-output data. These latter are assumed to be the result of many (measurable) inputs which can be highly correlated and possibly also poorly exciting. Such scenario is often encountered when modeling dynamic networks since modules interconnections give rise to feedback and algebraic loops [3], [9], [11], [14], [31], [39]. This complicates considerably the identification problem: low pass and almost collinear inputs lead to severely ill-conditioned estimation problems [5, Chapter 3] [7], as also described in many engineering applications like [17], [20], [29]. In addition, the use of the classical approach to system identification [18], [35], where different parametric structures have to be postulated, rises several difficulties. For instance, the use of rational transfer functions to describe each impulse

response lead to high-dimensional nonconvex optimization problems. In addition, system dimension has typically to be estimated from data, e.g. using AIC or cross validation [1], [13], and this further complicates the problem due to the combinatorial nature of model order selection.

The problem of collinearity in linear regression has been discussed for several decades [5], [36], [41]. Two types of methods are mainly considered. One consists of eliminating some related regressors, the other of exploiting special regression methods like LASSO, ridge regression or partial least squares [36]. The main idea underlying these approaches is to eliminate or decrease the influence of correlated variables. This strategy is useful when the goal is to obtain a model useful for predicting future data from inputs with statistics similar to those in the training set. In this paper, we instead follow a different route based on Bayesian identification of dynamic systems via Gaussian regression [4], [6], [27], [32]. In particular, we will couple the stable spline prior proposed in [24]–[26] with a Markov chain Monte Carlo (MCMC) strategy [10] suited to overcome collinearity. In particular, the stable spline kernel is a nonparametric description of stable systems which has shown some important advantages in comparison with classical parametric prediction error methods [18], [22], [27]. It includes information on smooth exponential decay and depends on two different kinds of hyperparameters: a scale factor and a common decay rate [2], [23], [28]. The main novelty in this paper is that the stable spline kernel will be implemented using a Full Bayes approach where the posterior of impulse responses is sampled through an MCMC strategy able to deal with collinearity. This is obtained by designing a variation of Gibbs sampling able to visit more frequently those parts of the parameter space more correlated.

The structure of the paper is as follows. Section II reports the problem statement by introducing the measurement model and the prior model on the unknown impulse responses. In Section III, we describe the system identification procedure, discussing issues regarding the selection of the overlapping blocks to be updated during the MCMC simulation and the impact of stable spline scale factors on the estimation performance. Section IV illustrates two numerical examples. Conclusions then end the paper.

<sup>1</sup>Department of Automation, Shanghai Jiao Tong University, Shanghai, China. wenqicao@sjtu.edu.cn

<sup>2</sup>Department of Information Engineering, University of Padova, Padova, Italy. giapi@dei.unipd.it

## II. PROBLEM FORMULATION

The measurement model is

$$y_i = \sum_{k=1}^m F_k u_k + e_i, \quad i = 1, \dots, n \quad (1)$$

where the  $F_k$  are stable rational transfer functions sharing a common denominator,  $y_i$  is the output measured at  $t_i$  while  $u_k$  is the known input entering the  $k$ -th channel. Finally, the random variables  $e_i$  form a white Gaussian noise of variance  $\sigma^2$ . The problem is to estimate the  $m$  transfer functions from the input-output samples. The difficulties we want to face is that the number of unknown parameters can be relatively large w.r.t. the data set size  $n$  and some of the  $u_k$  may be highly correlated.

We rewrite (1) in matrix-vector form by assuming that FIR models of (possibly large) order  $p$  can well approximate each  $F_k$ . In particular,  $G_k \in \mathbb{R}^{n \times p}$  are suitable Toeplitz matrices containing past input values such that

$$Y = \left( \sum_{k=1}^m G_k \theta_k \right) + E = G\theta + E \quad (2)$$

where the column vectors  $Y, \theta_k$  and  $E$  contain, respectively, the  $n$  output measurements, the  $p$  impulse response coefficients defining the  $k$ -th impulse response and the  $n$  i.i.d. Gaussian noises. Finally, on the rhs  $G = [G_1 \dots G_m]$  while  $\theta$  is the column vector which contains all the  $\theta_k$ .

Following the Bayesian approach to linear system identification documented in [26], [27], for known covariance, the  $\theta_k$  are seen as Gaussian vectors with zero-mean and covariances proportional to the stable spline matrix  $K \in \mathbb{R}^{p \times p}$  that encodes smooth exponential decay information. In particular, the  $i, j$ -entry of  $K$  is

$$K(i, j) = \alpha^{\max(i, j)}. \quad (3)$$

where  $\alpha$  regulates how fast the impulse responses are expected to go to zero. This parameter will be assumed to be known in what follows to simplify exposition.

Differently from [26], the covariances of the  $\theta_k$  depend on scale factors  $\lambda_k$  which are seen as independent random variables following an improper Jeffrey's distribution [16]. Such prior in practice includes only nonnegativity information and is specified by

$$p(\lambda_k) \sim \frac{1}{\lambda_k} \quad (4)$$

where here, and in what follows,  $p(\cdot)$  denotes a probability density function. Later on, we will also see that constraining all the scale factors to be the same can be crucial to deal with collinearity. The noise variance  $\sigma^2$  is also a random variable (independent of the  $\lambda_k$ ) and follows the Jeffrey's prior. Finally, for known  $\lambda_k$  and  $\sigma^2$ , all the  $\theta_k$  and the noises in  $E$  are assumed mutually independent.

## III. GIBBS SAMPLING WITH OVERLAPPING BLOCKS

### A. Bayesian regularization

From Section II, one obtains

$$Y \mid (\{\theta_k\}, \{\lambda_k\}, \sigma^2) \sim \mathcal{N}(G\theta, \sigma^2 I), \quad (5a)$$

$$\theta_k \mid \lambda_k \sim \mathcal{N}(0, \lambda_k K), \quad (5b)$$

$$E \mid \sigma^2 \sim \mathcal{N}(0, \sigma^2 I). \quad (5c)$$

Using Bayes rule, one has

$$\lambda_k \mid (Y, \sigma^2, \{\theta_k\}, \{\lambda_j\}_{j \neq k}) \sim \mathcal{I}_g\left(\frac{p}{2}, \frac{1}{2} \theta_k' K^{-1} \theta_k\right), \quad (6a)$$

$$\sigma^2 \mid (Y, \{\theta_k\}, \{\lambda_k\}) \sim \mathcal{I}_g\left(\frac{n}{2}, \frac{\|Y - G\theta\|^2}{2}\right), \quad (6b)$$

$$\theta_k \mid (Y, \sigma^2, \{\lambda_k\}, \{\theta_j\}_{j \neq k}) \sim \mathcal{N}(\hat{\mu}_k, \hat{\Sigma}_k), \quad (6c)$$

where  $\mathcal{I}_g(\cdot, \cdot)$  denotes the inverse Gamma distribution,

$$\hat{\mu}_k = \hat{\Sigma}_k \frac{1}{\sigma^2} G_k' (Y - \sum_{j \neq k} G_j \theta_j), \quad (6d)$$

$$\hat{\Sigma}_k = (\lambda_k^{-1} K^{-1} + \frac{1}{\sigma^2} G_k' G_k)^{-1}. \quad (6e)$$

The above equations would already allow to implement a Gibbs sampling approach where, at any iteration  $t$ , the following samples are generated

$$\lambda_k^{(t)} \mid (Y, \sigma^{2(t-1)}, \{\lambda_j^{(t)}\}_{j=1}^{k-1}, \{\lambda_j^{(t-1)}\}_{j=k+1}^m, \{\theta_k^{(t-1)}\}), \quad \text{for } k = 1, \dots, m, \quad (7a)$$

$$\sigma^{2(t)} \mid (Y, \{\lambda_k^{(t)}\}, \{\theta_k^{(t-1)}\}), \quad \text{for } k = 1, \dots, m, \quad (7b)$$

$$\theta_k^{(t)} \mid (Y, \sigma^{2(t)}, \{\lambda_k^{(t)}\}, \{\theta_j^{(t)}\}_{j=1}^{k-1}, \{\theta_j^{(t-1)}\}_{j=k+1}^m), \quad \text{for } k = 1, \dots, m. \quad (7c)$$

However, such classical approach may have difficulties to handle collinearity, leading to slow mixing of the chain. This motivates the development described in the next sections.

### B. Overlapping blocks

In our system identification setting, collinearity is related to the relationship between two inputs  $u_i$  and  $u_j$ , making some posterior regions more difficult to be explored. We need a collinearity measure that allows our sampling strategy to focus more on these parts of the parameter space. In particular, we still generate samples of the single  $\theta_i$  according to the equations described above but we want also to update larger blocks containing couples of impulse responses which are significantly correlated a posteriori. A first important index is the absolute value of the correlation coefficient, i.e.

$$c_{ij} := \left| \frac{\text{Cov}(u_i, u_j)}{\sqrt{\text{Var}(u_i) \text{Var}(u_j)}} \right|, \quad (8)$$

where  $\text{Cov}(\cdot, \cdot)$  and  $\text{Var}(\cdot)$  denote covariance and variance, respectively. It is now crucial to define a suitable function which maps each  $c_{ij}$  into the probability to update the vector containing both  $\theta_i$  and  $\theta_j$  at once.

Formally, define  $\theta_{ij} := [\theta_i', \theta_j']'$  and let  $P_{ij}$  be the probability of selecting  $\theta_{ij}$  as the block to be updated inside an MCMC iteration. In particular, we will use an exponential rule that emphasises correlation coefficients close to one, i.e.

$$P_{ij} = \begin{cases} 0, & i = j; \\ \frac{e^{\beta c_{ij}} - 1}{\text{sum}}, & i \neq j; \end{cases} \quad (9)$$

where  $sum = \sum_{i < j} (e^{\beta c_{ij}} - 1)$ , and  $\beta$  is a tuning rate. For instance, the profile of  $P_{ij}$  as a function of  $c_{ij}$  for  $\beta = 20$  is displayed in Fig. 1.

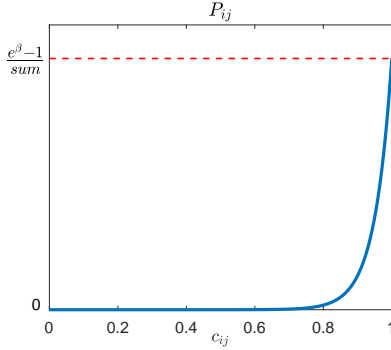


Fig. 1.  $P_{ij}$  with respect to  $c_{ij}$

Now, letting  $G_{ij} = [G_i, G_j]$ , the conditional distribution of  $\theta_{ij}$  is

$$\theta_{ij} | (Y, \sigma^2, \{\theta_k\}_{k \neq i,j}, \{\lambda_k\}) \sim \mathbf{N}(\hat{\mu}_{ij}, \hat{\Sigma}_{ij}) \quad (10a)$$

where

$$\hat{\Sigma}_{ij} = \begin{pmatrix} \lambda_i^{-1} K^{-1} & 0 \\ 0 & \lambda_j^{-1} K^{-1} \end{pmatrix} + \frac{1}{\sigma^2} G'_{ij} G_{ij}^{-1}, \quad (10b)$$

$$\hat{\mu}_{ij} = \hat{\Sigma}_{ij} \frac{1}{\sigma^2} G'_{ij} (Y - \sum_{k \neq i,j} G_k \theta_k). \quad (10c)$$

So, summarizing, our scheme updates all the parameters sequentially by using (7a-7c). But, in addition, according to  $P_{ij}$ , some larger impulse responses blocks are selected and updated. Following [10, Chapter 1.3], the acceptance rate of such overlapping blocks  $\theta_{ij}$  is always 1.

### C. A common scale factor

The simulation strategy described in the previous section uses a model where the covariance of each impulse response depends on a different scale factor  $\lambda_k$ . As described also by simulation results in Section IV, in presence of strong collinearity, such statistical description may make the chain nearly reducible [10, Chapter 3], i.e. unable to visit the highly correlated parts of the posterior. The problem can be overcome by reducing model complexity, i.e. assigning a common scale factor to all the impulse responses covariances. Hence, the distribution (6a) becomes

$$\lambda | (Y, \sigma^2, \{\theta_k\}) \sim \mathcal{I}_g\left(\frac{np}{2}, \frac{1}{2} \sum \theta'_k K^{-1} \theta_k\right) \quad (11)$$

and the update of  $\lambda$ , previously define by (7a), becomes

$$\lambda^{(t)} | (Y, \sigma^{2(t-1)}, \{\theta_k^{(t-1)}\}). \quad (12)$$

Hence, at step  $t$  of the MCMC algorithm, when  $\theta_{ij}$  is selected it is updated according to

$$\theta_{ij}^{(t)} | (Y, \sigma^{2(t)}, \lambda^{(t)}, \{\theta_k^{(t)}\}_{k \neq i,j}), \quad (13)$$

i.e. using (10) with  $\lambda_i = \lambda_j = \lambda^{(t)}$ . We are now in a position to introduce our MCMC strategy for linear system

---

**Algorithm 1** Gibbs samplings with overlapping blocks using one common scale factor (GSOB)

---

**Input:** Measurements  $G, Y$ ; initial values  $\lambda^{(0)}, \sigma^{2(0)}, \{\theta_k^{(0)}\}, \alpha, \beta$ .

**Output:** Estimate  $\hat{\theta}$ .

- 1: Calculate  $\{P_{ij}\}$  from input data for  $i \leq j$  in (9);
  - 2: **for**  $t = 1 : n_{MC}$  **do**
  - 3:   Sample (12), (7b) and (7c) in sequence;
  - 4:   **for**  $k = 1 : n_{OB}$  **do**
  - 5:     Choose a pair  $(i, j)$  from the distribution  $\{P_{ij}\}_{i \leq j}$ ;
  - 6:     Sample (13) and update the values of  $\theta_i^{(t)}$  and  $\theta_j^{(t)}$ .
  - 7:   **end for**
  - 8: **end for**
  - 9: Calculate  $\hat{\theta}$  as the mean of the impulse responses samples from  $t = n_B + 1$  to  $t = n_{MC}$ .
- 

identification under collinear inputs, which relies on Gibbs samplings with overlapping blocks (GSOB). Using  $n_{MC}$  to indicate the number of MCMC steps,  $n_{OB}$  the number of overlapping blocks which were selected and updated at each iteration, and  $n_B$  the number of burn-in [10, Chapter 7], such procedure is summarized in Algorithm 1.

## IV. SIMULATION EXAMPLES

### A. Example 1

In the first example we shall use one extreme case with two inputs that are exactly the same. This will illustrate the difficulties due to collinearity, as well as the importance of adopting only a common scale factor  $\lambda$  for all the impulse responses.

Let  $u_1(t) = u_2(t)$ , with the inputs defined by realizations of white Gaussian noise with  $n = 500$ . We consider two randomly generated transfer functions  $F_1(z), F_2(z)$  with a common denominators of degree 5, displayed e.g. in the two panels of Fig. 2. The measurement noises  $e_i$  are independent Gaussians of variance 0.3. In the Fisherian framework used by classical system identification this problem is non-identifiable. But we use model (2) of order  $p = 50$  and the Bayesian framework to find impulse responses estimates. In this experiment, and in all the other ones, we set  $\alpha = 0.9$ .

In this example,  $c_{12} = c_{21} = 1$ , so that  $P_{12} = P_{21} = 1$  after normalization. We run  $n_{MC} = 500$  Monte-Carlo iterations in MATLAB to compare the following four algorithms:

- GSOB: Gibbs sampling with overlapping blocks using the same scale factor with  $n_{OB} = 2$ ;
- GSOBd: Gibbs sampling with overlapping blocks using different scale factors  $n_{OB} = 2$ ;
- GS: Gibbs sampling without overlapping blocks using the same scale factor;
- GSd: Gibbs sampling without overlapping blocks using different scale factors.

The posterior of the two impulse responses is reconstructed using samples from MCMC considering the first 50% as burn-in. Results coming from the four procedures are displayed in Figs. 2, 3, 4 and 5 (true impulse responses are the red thick lines).

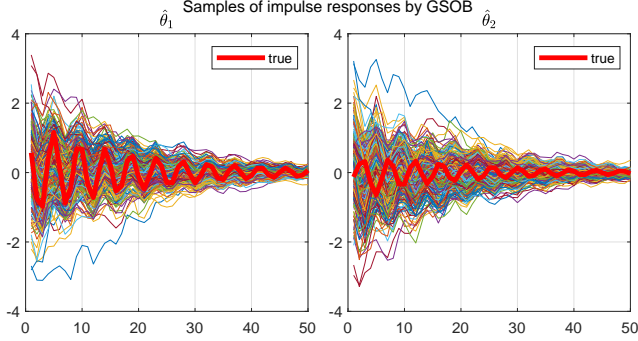


Fig. 2. Samples of impulse responses after 500 iterations of algorithm GSOB in Example 1.

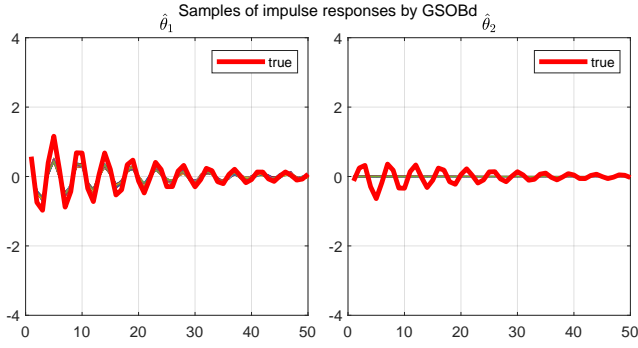


Fig. 3. Samples of impulse responses after 500 iterations of algorithm GSOBd in Example 1.

After the 500 iterations, only GSOB returns a sampled version of the posterior able to highlight the non-identifiability issues underlying the problem, see Fig. 2. Results from classical Gibbs sampling are in Fig. 4. One can see that samples of  $\theta_2$  have not yet reached the same informativeness of GSOB. The reason is that GS converges much slower than GSOB under collinearity.

The situation is even more critical when adopting different scale factors. In fact, Figs. 3 and 5 show that the samples of the second impulse response  $\theta_2$  are all close to zero. The reason is that chains with multiple scale factors may easily become nearly reducible. At the first MCMC iterations, the algorithm generates an impulse response  $\theta_1$  able to explain all the data. Hence,  $\theta_2$  is virtually set to zero and then also  $\lambda_2$  becomes very small. This scale factor becomes a strong (and wrong) prior for  $\theta_2$  during the next iterations, always suggesting the sampler use only  $\theta_1$  to fit the output data.

### B. Example 2

In this example we shall use 100 inputs to test the appearance of our algorithm when facing large-scale systems. This

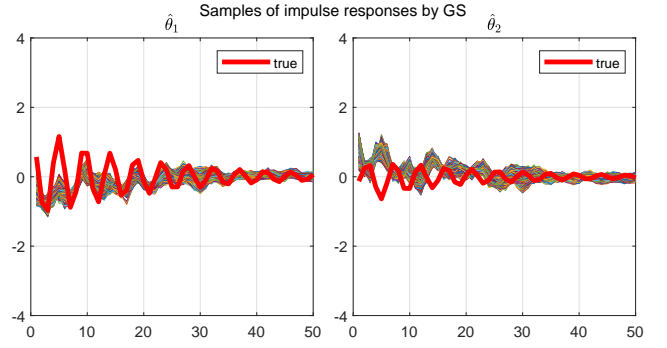


Fig. 4. Samples of impulse responses after 500 iterations of algorithm GS in Example 1.

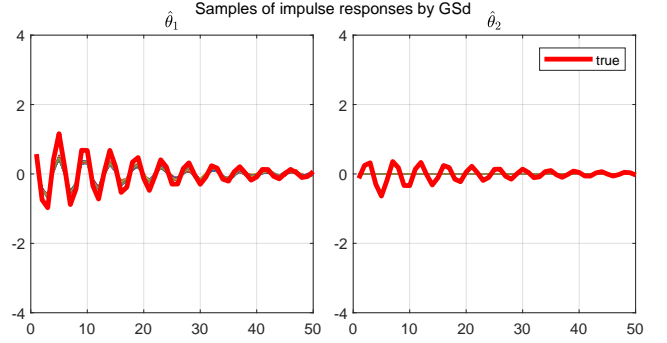


Fig. 5. Samples of impulse responses after 500 iterations of algorithm GSd in Example 1.

is a situation where dividing the parameter space into many small blocks can have crucial computational advantages. Otherwise, one should deal with inversion of very large matrices whose dimension is the overall number of impulse response coefficients.

We generate collinear inputs as follows

$$u_i(t) = u_j(t) + r_{ij}(t), \quad (14)$$

where  $r_{ij}(t)$  is a noise independent of  $u_j$ . To increase collinearity between inputs, and the ill-conditioning affecting the problem,  $r_{ij}(t)$  in (14) is a moving average (MA) process,

$$r_{ij}(t) = v_{ij}(t) - 0.8v_{ij}(t-1),$$

where  $v_{ij}(t) \sim \mathcal{N}(0, \gamma_{ij}^2)$ . From (8), one has

$$c_{ij} = \frac{1}{\sqrt{1 + \gamma_{ij}^2/(1 - 0.8^2)}},$$

when  $u_j(t)$  is a zero mean process with variance 1. The level of collinearity can then be tuned by  $\gamma_{ij}$ .

Data set size is set to  $n = 10^5$ . We introduce correlation to 10% of the inputs by letting

$$u_{i+1}(t) = u_i(t) + r_{(i+1)i}(t), \quad (15)$$

for  $i = 1, \dots, 9$ , where the first input  $u_1(t)$  is white and Gaussian of variance one,  $r_{(i+1)i}(t)$  is obtained by setting

the  $c_{i(i+1)} = 0.99$  for  $i = 1, 2, \dots, 9$ . The other 90% of the inputs, i.e.  $\{u_i\}_{i=11}^{100}$  are zero-mean standard i.i.d. Gaussian processes.

The different collinearity levels of the first 10 inputs are summarized by the correlation coefficient matrix (approximately calculated from the input realizations) reported in Fig. 6. One can see that the input pairs have correlation coefficients ranging from 0.99 to 0.92.

We set  $\beta = 100$  and then we use (9) to compute the probabilities of selecting the overlapping blocks.  $P_{ij}$  for the first 10 impulse responses are shown in Fig. 7 (a) with a sharing colorbar at the bottom ( $P_{ij}$  for  $i, j > 10$  are obviously all close to zero). In all pairs considered for constructing overlapping blocks  $(i, j)$  ( $i \neq j$ ). The couples  $(i, i + 1)$  ( $i = 1, \dots, 9$ ) of highest collinearity are assigned almost 7% of the total amount of probability. On the other hand, e.g. the couple  $(1, 10)$ , which has a correlation coefficient 0.9205, is given 0.0063%.

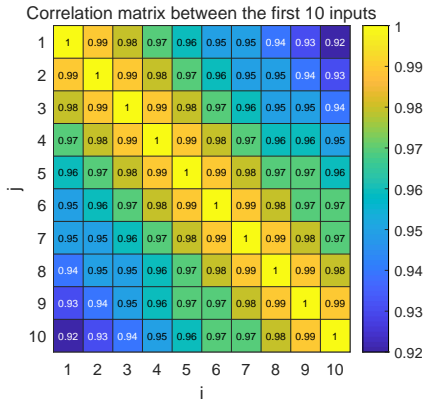


Fig. 6.  $\{c_{ij}\}$  of  $\{(u_i, u_j)\}_{i,j=1}^{10}$  in Example 2.

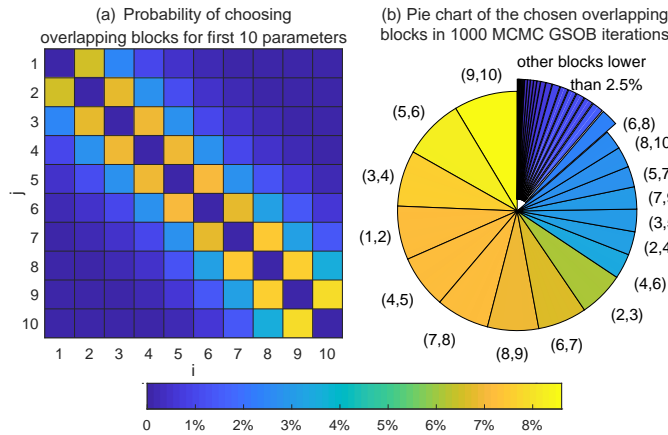


Fig. 7. (a) Probability  $\{P_{ij}\}$  of choosing couples  $\{(i, j)\}_{i,j=1}^{10}$  in example 2 of GSOB; (b) pie chart of the selected frequencies of overlapping blocks in 1000 Gibbs iterations of GSOB in Example 2.

We generate random transfer functions  $F_i(z)$  ( $i = 1, \dots, 100$ ) of degree 5 with a common denominator. Measurement Gaussian noises  $e_i$  have variance 0.3. We adopt model (2) with each impulse response of order  $p = 50$

and show results coming only from GSOB and GS, letting  $\alpha = 0.9$ ,  $n_{OB} = 10$  and  $n_{MC} = 1000$ . The pie chart of the selected overlapping blocks' index pairs is shown in Fig. 7 (b), where the frequencies of selection of the overlapping blocks are shown in different colors. As expected, they turn out close to the probabilities  $P_{ij}$ . More correlated the pair  $(i, j)$  is, more times it is sampled.

The last 50% of MCMC realizations are used to reconstruct the impulse responses posterior in sampled form, as done in Example 1. Results concerning the first 10 impulse responses (related to the strongly collinear inputs) are shown in Fig. 8. One can see that GSOB works better than GS. For readers' convenience, samples from the posterior of  $\theta_1$  and  $\theta_3$  are also zoomed. Regarding the other impulse responses (related to inputs which are mutually independent) the performance of both the algorithms is similar, e.g. samples of  $\{\theta_i\}_{i=61}^{70}$  are visible in Fig. 9.

Another fundamental feature of GSOB is its better convergence rate w.r.t. GS. This can be appreciated e.g. by analyzing the samples from the posterior of the scale factor  $\lambda$  generated by these two procedures. They are shown in Fig. 10, as a function of the first 250 iterations. Chain's mixing of GSOB is significantly faster than GS.

## V. CONCLUSION

Identification of large-scale linear dynamic systems may be subject to two relevant problems. First, the number of unknown variables to estimate may be large. Using an MCMC scheme to reconstruct the posterior of the impulse response coefficients given the identification data, this means that any step of the algorithm can be computationally expensive (a matrix of very large dimension has to be inverted to draw samples from the full conditional distributions of  $\theta$ ). Hence, it is important to derive schemes where small groups of variables are updated. In addition, ill-conditioning can affect the problem due to input collinearity which can also lead to slow mixing of the generated Markov chains. This aspect requires a careful selection of the blocks to be updated. An MCMC strategy based on the stable spline prior has been here proposed that addresses both of the above issues. It relies on Gibbs sampling complemented with a strategy where overlapping blocks are updated. The updating frequency of such blocks is regulated by the level of collinearity among different system inputs. Simulation results show good performance of the proposed algorithm. In future work we plan to provide a theoretical analysis regarding the convergence of the proposed MCMC scheme which will require to extend previous studies on Gibbs sampling like that reported in [33], [34], [38].

## REFERENCES

- [1] H. Akaike, "A new look at the statistical model identification," *IEEE Trans. on Automatic Control*, vol. AC-19, pp. 716–723, 1974.
- [2] A. Aravkin, J. Burke, A. Chiuso, and G. Pillonetto, "On the estimation of hyperparameters for empirical bayes estimators: Maximum marginal likelihood vs minimum mse," *IFAC Proceedings Volumes*, vol. 45, no. 16, pp. 125 – 130, 2012.

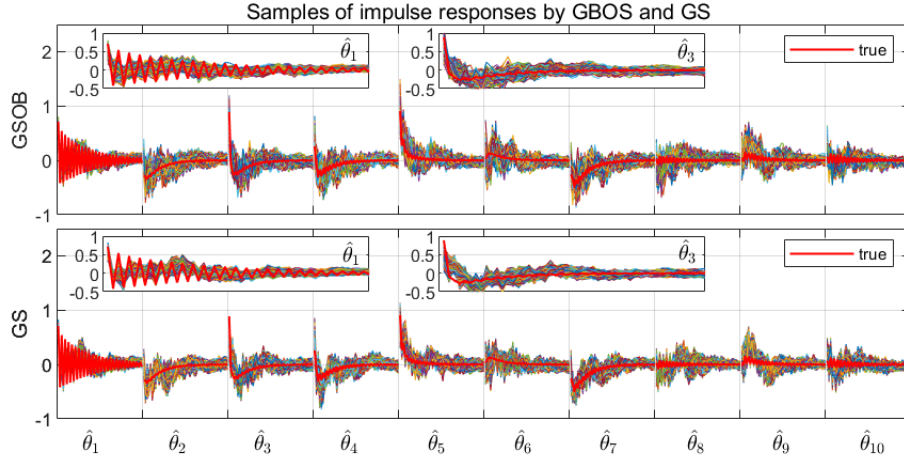


Fig. 8. Sampled impulse responses of  $\{\theta\}_{i=1}^{10}$  after 1000 iterations of algorithms GSOB and GS in Example 2.

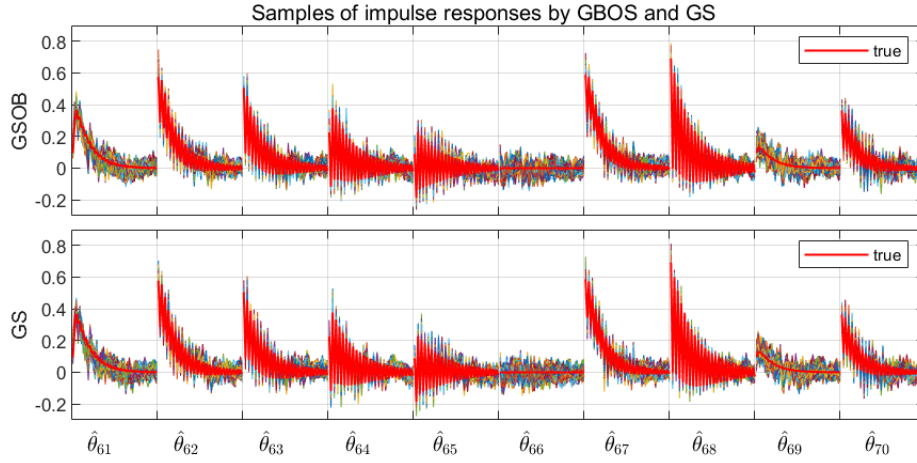


Fig. 9. Sampled impulse responses of  $\{\theta\}_{i=61}^{70}$  after 1000 iterations of algorithms GSOB and GS in Example 2.

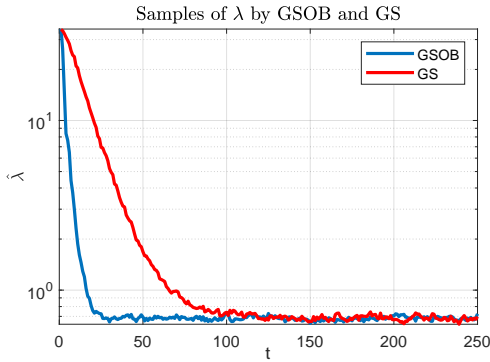


Fig. 10. Samples of  $\lambda$  in the first 250 iterations by GSOB and GS in Example 2.

- [3] A. Bazanella, M. Gevers, J. Hendrickx, and A. Parraga, "Identifiability of dynamical networks: Which nodes need be measured?" in *2017 IEEE 56th Annual Conference on Decision and Control (CDC)*, 2017, pp. 5870–5875.
- [4] B. Bell and G. Pillonetto, "Estimating parameters and stochastic functions of one variable using nonlinear measurement models," *Inverse*

- Problems*, vol. 20, no. 3, p. 627, 2004.
- [5] D. A. Belsley and R. E. Welsch, *Regression Diagnostics: Identifying Influential Data and Sources of Collinearity*. New York: Wiley, 1980.
- [6] G. Bottegal, H. Hjalmarsson, and G. Pillonetto, "A new kernel-based approach to system identification with quantized output data," *Automatica*, vol. 85, pp. 145–152, 2017.
- [7] A. Chiuso and G. Picci, "On the ill-conditioning of subspace identification with inputs," *Automatica*, vol. 40, no. 4, pp. 575–589, 2004.
- [8] A. Chiuso and G. Pillonetto, "A Bayesian approach to sparse dynamic network identification," *Automatica*, vol. 48, no. 8, pp. 1553–1565, 2012.
- [9] S. Fonken, M. Ferizbegovic, and H. Hjalmarsson, "Consistent identification of dynamic networks subject to white noise using weighted null-space fitting," in *Proc. 21st IFAC World Congress, Berlin, Germany*, 2020.
- [10] W. Gilks, S. Richardson, and D. Spiegelhalter, *Markov chain Monte Carlo in Practice*. London: Chapman and Hall, 1996.
- [11] J. Goncalves and S. Warnick, "Necessary and sufficient conditions for dynamical structure reconstruction of lti networks," *IEEE Transactions on Automatic Control*, vol. 53, no. 7, pp. 1670–1674, 2008.
- [12] P. Hagmann, L. Cammoun, X. Gigandet, R. Meuli, C. Honey, V. Wedeen, and O. Sporns, "Mapping the structural core of human cerebral cortex," *PLOS Biology*, vol. 6, no. 7, pp. 1–15, 2008.
- [13] T. J. Hastie, R. J. Tibshirani, and J. Friedman, *The Elements of Statistical Learning. Data Mining, Inference and Prediction*. Canada: Springer, 2001.
- [14] J. Hendrickx, M. Gevers, and A. Bazanella, "Identifiability of dynamical systems," *Automatica*, vol. 40, no. 3, pp. 307–318, 2004.

- ical networks with partial node measurements," *IEEE Transactions on Automatic Control*, vol. 64, no. 6, pp. 2240–2253, 2019.
- [15] R. Hickman, M. V. Verk, A. Van Dijken, M. Mendes, I. A. Vroegop-Vos, L. Caarls, M. Steenberg, I. Van der Nagel, G. Wesselink, A. Jironkin, A. Talbot, J. Rhodes, M. De Vries, R. Schuurink, K. Denby, C. Pieterse, and S. Van Wees, "Architecture and dynamics of the jasmonic acid gene regulatory network," *The Plant Cell*, vol. 29, no. 9, pp. 2086–2105, 2017.
- [16] H. Jeffreys, "An invariant form for the prior probability in estimation problems," *Proc. R. Soc. Lond.*, vol. 186, pp. 453–461, 1946.
- [17] S. Liverani, A. Lavigne, and M. Blangiardo, "Modelling collinear and spatially correlated data," *Spatial and Spatio-temporal Epidemiology*, vol. 18, pp. 63–73, 2016.
- [18] L. Ljung, *System Identification - Theory for the User*, 2nd ed. Upper Saddle River, N.J.: Prentice-Hall, 1999.
- [19] D. Materassi and G. Innocenti, "Topological identification in networks of dynamical systems," *IEEE Transactions on Automatic Control*, vol. 55, no. 8, pp. 1860–1871, 2010.
- [20] J. Molitor, M. Papatomas, M. Jerrett, and S. Richardson, "Bayesian profile regression with an application to the national survey of children's health," *Biostatistics*, vol. 11, no. 3, pp. 484–498, July 2010.
- [21] G. Pagani and M. Aiello, "The power grid as a complex network: A survey," *Physica A: Statistical Mechanics and its Applications*, vol. 392, no. 11, pp. 2688–2700, 2013.
- [22] G. Pillonetto, T. Chen, A. Chiuso, G. D. Nicolao, and L. Ljung, *Regularized System Identification*. Springer, 2022.
- [23] G. Pillonetto and A. Chiuso, "Tuning complexity in regularized kernel-based regression and linear system identification: The robustness of the marginal likelihood estimator," *Automatica*, vol. 58, pp. 106 – 117, 2015.
- [24] G. Pillonetto, A. Chiuso, and G. De Nicolao, "Regularized estimation of sums of exponentials in spaces generated by stable spline kernels," in *Proceedings of the IEEE American Cont. Conf., Baltimore, USA*, 2010.
- [25] —, "Prediction error identification of linear systems: a nonparametric Gaussian regression approach," *Automatica*, vol. 47, no. 2, pp. 291–305, 2011.
- [26] G. Pillonetto and G. De Nicolao, "A new kernel-based approach for linear system identification," *Automatica*, vol. 46, no. 1, pp. 81–93, 2010.
- [27] G. Pillonetto, F. Dinuzzo, T. Chen, G. D. Nicolao, and L. Ljung, "Kernel methods in system identification, machine learning and function estimation: a survey," *Automatica*, vol. 50, no. 3, pp. 657–682, 2014.
- [28] G. Pillonetto and A. Scampicchio, "Sample complexity and minimax properties of exponentially stable regularized estimators," *IEEE Trans. Automat. Contr.*, 2021.
- [29] A. Pitard and J. F. Viel, "Some methods to address collinearity among pollutants in epidemiological time series," *Statistics in Medicine*, vol. 16, no. 5, pp. 527–544, 1997.
- [30] G. Prando, M. Zorzi, A. Bertoldo, M. Corbetta, M. Zorzi, and A. Chiuso, "Sparse dcm for whole-brain effective connectivity from resting-state fmri data," *NeuroImage*, vol. 208, p. 116367, 2020.
- [31] K. Ramaswamy and P. J. Van den Hof, "A local direct method for module identification in dynamic networks with correlated noise," *IEEE Transactions on Automatic Control*, 2021.
- [32] C. Rasmussen and C. Williams, *Gaussian Processes for Machine Learning*. The MIT Press, 2006.
- [33] C. P. Robert, "Convergence control methods for markov chain monte carlo algorithms," *Statistical Science*, vol. 10, no. 3, pp. 231–253, 1995.
- [34] G. O. Roberts and S. K. Sahu, "Updating schemes, correlation structure, blocking and parameterization for the gibbs sampler," *Journal of the Royal Statistical Society*, vol. 59, no. 2, pp. 291–317, 1997.
- [35] T. Söderström and P. Stoica, *System Identification*. Prentice-Hall, 1989.
- [36] C. Srisa-An, "Guideline of collinearity - avoidable regression models on time-series analysis," in *2021 2nd International Conference on Big Data Analytics and Practices (IBDAP)*, 2021, pp. 28–32.
- [37] P. Van den Hof, A. Dankers, P. Heuberger, and X. Bombois, "Identification of dynamic models in complex networks with prediction error methods: basic methods for consistent module estimates," *Automatica*, vol. 49, no. 10, pp. 2994–3006, 2013.
- [38] N. Y. Wang and L. Wu, "Convergence rate and concentration inequalities for gibbs sampling in high dimension," *Bernoulli*, vol. 20, no. 4, pp. 1698–1716, 2014.
- [39] H. Weerts, P. J. Van den Hof, and A. Dankers, "Prediction error identification of linear dynamic networks with rank-reduced noise," *Automatica*, vol. 98, pp. 256–268, 2018.
- [40] Z. Yue, J. Thunberg, W. Pan, L. Ljung, and J. Goncalves, "Dynamic network reconstruction from heterogeneous datasets," *Automatica*, vol. 123, p. 109339, 2021.
- [41] J. Zhang, Z. Wang, X. Zheng, L. Guan, and C. Y. Chung, "Locally weighted ridge regression for power system online sensitivity identification considering data collinearity," *IEEE Transactions on Power Systems*, vol. 33, no. 2, pp. 1624–1634, March 2018.